08
Storm Surge

Storm Surge

8.1 Background

Associated with extreme winds, heavy rainfall and storm surge, land-falling tropical cyclones that are formed in the North Indian Ocean (NIO) region, often cause immense death and destruction in vulnerable coasts. Usually, much of the death toll and damage to property in coastal areas is as a result of cyclone-induced storm surge causing inundation of low-lying onshore lands (Dube, 2003, Lin et al 2010).

Sri Lanka, an island nation located off the southern tip of India, is vulnerable to cyclones generated mostly in southern part of Bay of Bengal, and to a lesser extent, to those in southeast of Arabian Sea. The cyclones which form over the southernmost part of Bay of Bengal at low latitudes mainly move west or west-north-westwards into the Gulf of Mannar across the coast of Sri Lanka. These cyclones generally form during the later part of the post-monsoon season or early part of the winter and pre-monsoon season. On the other hand, cyclones that form over Arabian Sea mostly move north or north-easterly whilst a few travel west or north-westwards (SAARC 1998).

However, owing to atmospheric dynamics associated with cyclones and the relative proximity of Sri Lanka to the equator, a large proportion of cyclones generated in Bay of Bengal and Arabian Sea, fortunately, do not make landfall in Sri

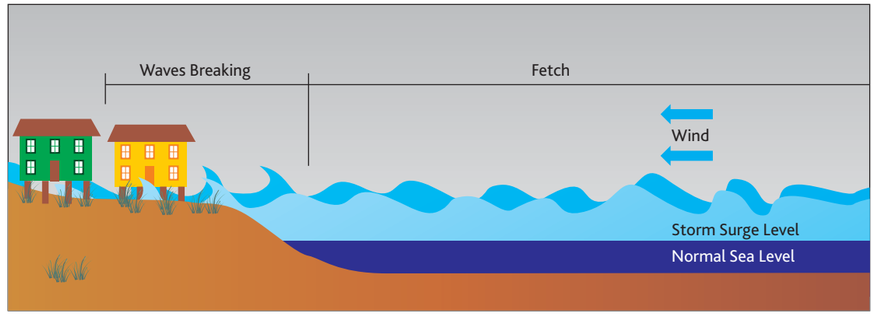

Fig 8.1 Storm surge- Schematic diagram (Source: www.hcfcd.org/tropicalweather)

Lanka. Yet, sixteen cyclonic or severe cyclonic storms have made landfall in Sri Lanka during the last century according to the Department of Meteorology, Sri Lanka (2010); some of these, the severe cyclonic storms in particular, have resulted in loss of lives of the order of several hundred as well as considerable damage to housing and other infrastructure due to both the surge and the high winds.

8.1.1 Causative Factors

Unlike the tsunami waves, which originate at the ocean floor, storm surge is caused primarily by high winds pushing on the ocean's surface and it is a surface phenomenon. It makes unusual rise in water level, due to piling up of sea water higher than the ordinary sea level caused by forces generated from a severe storm's wind, waves, and low atmospheric pressure at the centre of the weather system. It is extremely dangerous, because they are capable of flooding large coastal areas.

The height of the storm surge depends on cyclone dynamics such as the wind speed, the translation speed, the angle of attack at landfall, the pressure drop and also on coastal and shelf morphological factors such as the bathymetry and the shape of the coastline (Jelesnianski et al 1992). Further, the severity and the extent of onshore inundation depend primarily upon the surge height and the prevailing tide as well as the elevation, the slope and the surface roughness of the terrain.

8.1.2 Cyclonic Storms in North Indian Ocean

8.1.2.1 Origin & Movement

Tropical cyclones in the North Indian Ocean (NIO) region originate in either the Bay of Bengal or the Arabian Sea (Fig. 8.1.1). The Bay of Bengal cyclones which cross Bangladesh and adjoining West Bengal coast of India move in the north or northeasterly direction; and the cyclones

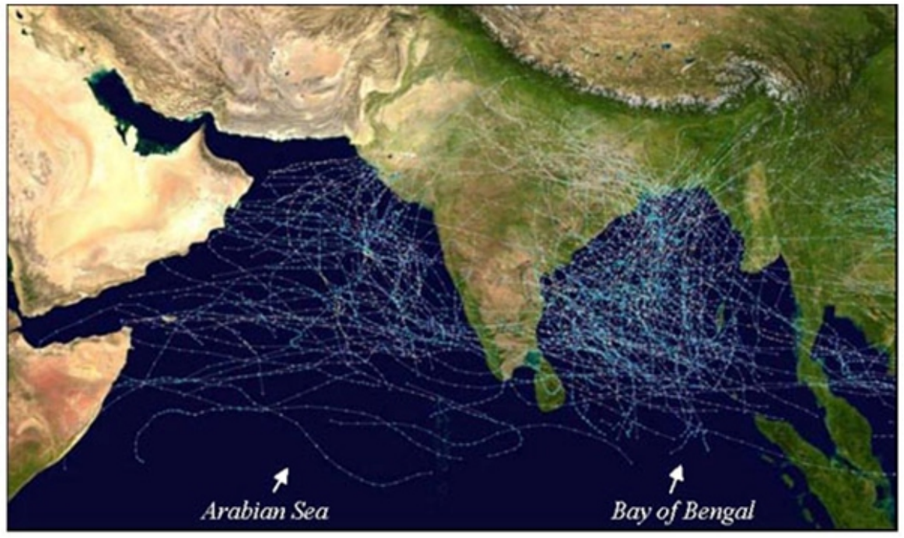

Fig. 8.1.1 Cumulative track map of all North Indian Ocean cyclones from 1970 to 2005

which cross the eastern coast of India move in westerly or northwesterly direction and sometimes re-curve northeastwards. Arabian Sea cyclones, which cross the coastal regions of India and Pakistan, generally move in the northeasterly or northerly direction over India and northerly or north-northeasterly direction over Pakistan. Some of the cyclones forming over the Arabian Sea move west or northwestwards up to African coasts (SAARC. 1998).

The cyclones which form over the southernmost Bay of Bengal at low latitudes mainly move west or west-northwestwards towards the Gulf of Mannar across the coast of Sri Lanka. These disturbances over the Gulf of Mannar intensify further and move in a west-northwesterly direction and finally make landfall at the Indian peninsula. A very few cyclones form over Laccadives Sea, which either make landfall at western coast of Sri Lanka or move in a westerly direction over the Arabian Sea.

A number of cyclones from the Bay of Bengal cross eastern coast of India into the land and weaken into a depression or into a low pressure system. These disturbances pass over India and emerge into the Arabian Sea. Most of them again move as tropical cyclones whilst some dissipate there (SAARC, 1998).

8.1.2.2 Period of Occurrence

As illustrated in Fig 8.2, these cyclones generally form in the early part of the winter and pre-southwest monsoon season (April-May) and during the later part of the post-southwest monsoon season (October-December) as indicated in SAARC (1998) & Kariyawasam (2005).

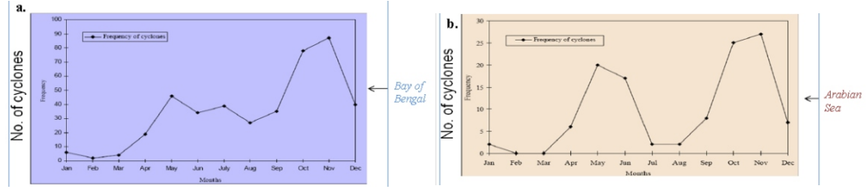

Fig 8.2 Temporal distribution of cyclonic storms and severe cyclonic storms in the North Indian Ocean during the period from 1891 to 1991: a) In Bay of Bengal, and b) In Arabian Sea4.

8.1.2.3 Frequency

During the period from 1891 to 2000, about 450 cyclones have formed in the Bay of Bengal and about 120 in the Arabian Sea. Of the 450 cyclones that formed in the Bay of Bengal during the period from 1891 to 2000, 57% have made landfall in India, 16% in Bangladesh, 8% in Myanmar, 4% in Sri Lanka, whilst the remaining 15% have dissipated over the ocean.

Apart from that 1/4th of the cyclones that formed in the Bay of Bengal during the above period were very severe cyclonic storms (with maximum velocity exceeding 118 km/h) and made landfall as follows: 52% in India, 25% in Bangladesh, 10% in Myanmar, 2% in Sri Lanka, and the remaining 11% have dissipated over the ocean (SAARC 1998).

8.1.3 Cyclones that Made Landfall in Sri Lanka

A brief review of notable past cyclones that made landfall in Sri Lanka during the past 130 years is given in Table 8.1. According to the classification of revolving tropical systems adopted in Sri Lanka (Table 8.1), maximum sustained wind speeds of 62-88 km/h and 89-118 km/h are categorized as cyclonic storms and severe cyclonic storms, respectively (Department of Meteorology, Sri Lanka,2010).

Sixteen cyclones, of which 5 are notable severe cyclonic storms (occurred in 1964 Dec, 1978 Nov, 1931 Dec, 1922 Nov, and 1907 March), are known to have crossed

Table 8.1 Classification of tropical cyclonic systems in Sri Lanka (Source: Department of Meteorology, Sri Lanka 2010)

Weather System	Maximum Sustained Wind Speed (km/h)
Low pressure area	< 31
Depression	31 -61
Cyclonic storm	62 -88
Severe cyclonic storm	89 -118
Very severe cyclonic storm	119 -221
Super cyclonic storm	> 222

Table 8.2 Past cyclones that made landfall in Sri Lanka during 1881-2000- (Source: Department of Meteorology, Sri Lanka 2010).

Cyclone No.	Year/Month	Classification	Formed in	Landfall
1	1906 Jan	Cyclonic Storm	Bay of Bengal	North
2	1907 March	Severe Cyclonic Storm	Bay of Bengal	East
3	1908 Dec	Cyclonic Storm	Bay of Bengal	North
4	1912 Dec	Cyclonic Storm	Bay of Bengal	South
5	1913 Dec	Cyclonic Storm	Bay of Bengal	South East
6	1919 Dec	Cyclonic Storm	Bay of Bengal	North
7	1922 Nov	Severe Cyclonic Storm	Bay of Bengal	East
8	1925 March	Cyclonic Storm	Arabian Sea	North West
9	1931 Dec	Severe Cyclonic Storm	Bay of Bengal	North
10	1964 Dec	Severe Cyclonic Storm	Bay of Bengal	East
11	1966 Nov	Cyclonic Storm	Bay of Bengal	East
12	1967 Dec	Cyclonic Storm	Arabian Sea	West
13	1978 Nov	Severe Cyclonic Storm	Bay of Bengal	East
14	1980 Dec	Cyclonic Storm	Bay of Bengal	East
15	1992 Dec	Severe Cyclonic Storm	Bay of Bengal	South East
16	2000 Dec	Severe Cyclonic Storm	Bay of Bengal	East

Sri Lanka during the past 130 years (Table 8.1 and Fig. 8.3). Table 8.2 also gives the general area of formation of these cyclones as well as the coastal region of Sri Lanka where each cyclone made landfall. Out of the 16 cyclones that crossed Sri Lanka during the past 130 years, only two have been formed in Arabian Sea and made landfall in either western or north-western coastlines of Sri Lanka; the rest have all been formed in Bay of Bengal and made landfall on the north and east coasts.

The monthly distribution of tropical cyclones that made landfall in Sri Lanka since 1881 (Fig. 8.4) indicates that over 80% of those cyclones have occurred during the period November-December. Consequently, November and December are considered as cyclone prone months for Sri Lanka (Department of Meteorology, Sri Lanka, 2010).

Of the severe cyclonic storms (Table 8.2), the systems that developed in December 1964 and November 1978 appear to have caused the most notable death and destruction;only little information is available on the impact in terms of number of casualties and damage to property due to the severe cyclonic

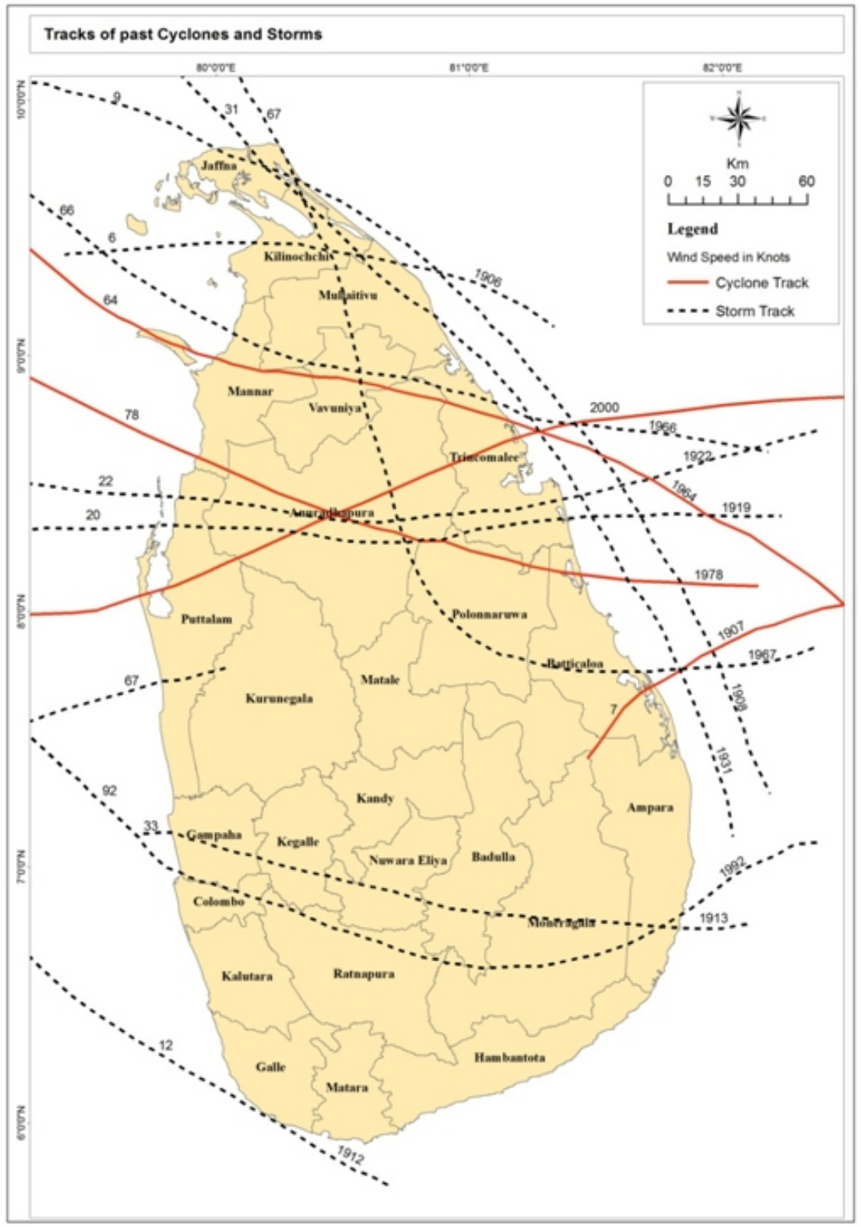

Fig 8.3 Tracks of past cyclones that made landfall in Sri Lanka during 1881-2000- (source: IRI 2011).

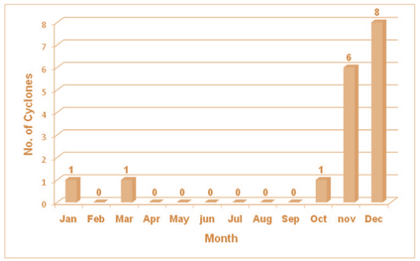

Fig 8.4 Monthly distribution of number of tropical cyclones that made landfall in Sri Lanka since 1881 (source: Department of Meteorology, Sri Lanka 2010).

storms that crossed Sri Lanka in 1907, 1922 and 1931.

The severe cyclonic storm that made landfall near Trincomalee on 23 December 1964 with reported maximum wind speeds of 216 km/h (about 220-240 km/h according to Kulshrestha et al , (1966), and Dinamina newspaper of 25th December 1964) resulted in a death toll of 842 and 100 missing according to Longshore, (2008) and about 650 deaths and 400 missing according to Dinamina newspaper of 25th December (1964) in the northern province including the city of Mannar in the northwest where a storm surge of height up to about 4.5 m (15 feet, Ceylon Daily Mirror issued on 29th December 1964) inundated and destroyed low-lying coastal settlements. Moreover, the 1964 cyclone is quite remarkable because it not only formed at a low latitude of 5°N but also attained the intensity of a severe cyclonic storm at about the same latitude (Kulshrestha et al, 1966).

The severe cyclonic storm that made landfall near Batticaloa on 24th November 1978 with satellite estimated maximum wind speeds of 222 km/h (Department of Meteorology, Sri Lanka, 2010) caused loss of lives as well as extensive damage to housing and buildings and generated a storm surge of height 1-2 m near Batticaloa with inland penetration of inundation reaching 1.5 km in Kalkudah (Department of Meteorology, Sri Lanka, 2010) The death toll attributed to this cyclone varies from 150 (Longshore, 2008). to 323 (Murty et al 1986) and 915 (Department of Meteorology, Sri Lanka, 2010); moreover, 185,000 housing units were severely damaged with another 150,000 partially damaged (Department of Meteorology, Sri Lanka, 2010).

The death toll due to the severe cyclonic storm that made landfall on 12th November 1992 was only 4, with over 29,000 housing units damaged. The severe cyclonic storm that crossed Sri Lanka on 26 December 2000 also resulted in 8 deaths and considerable property damage (Department of Meteorology, Sri Lanka, 2010).

The casualty and damage figures given above are usually due to the combined influence of one or more of the following cyclone related effects: storm surge, high winds, and heavy rainfall.

8.2 Scope of the Study

The scope of this study is to evaluate and map the distribution of the tropical cyclone induced storm surge hazard inclusive of the probable extent of onshore inundation for the entire coastline of Sri Lanka. Information gathered from the present assessment would provide the basis for disaster risk mitigation policy planning and decision making with regard to the cyclonic storm surge hazard for Sri Lanka.

The study consists of assessment of the cyclonic storm surge hazard for Sri Lanka including mapping of onshore inundation. The hazard assessment, which is based on a statistical analysis of the past cyclone events in Bay of Bengal and Arabian Sea during the last century, utilizes a numerical model based on depth-averaged, nonlinear equations of conservation of mass and momentum to simulate the storm surges due to several probable cyclone scenarios. Given the considerable uncertainty on the probable cyclone tracks including the landfall location, the storm surge simulations for each scenario are carried out for a large set of synthetic tracks that are in statistical agreement with the historical database in order to produce composite maps of the distribution of peak surge heights. GIS based modeling tools and supplementary software will be used to map the likely inundation distribution onshore based on the computed surge heights at the coastline.

8.3 Methodology

Methodology section concentrate on the availability of data & data gaps in the study, statistical analysis and different scenarios considered, numerical modelling, model verification for three severe cyclones, and mapping scales.

8.3.1 Data Availability

The primary data required for the present storm surge hazard assessment include topographic and bathymetric data pertinent to Sri Lanka as well as records of past cyclone events in the Bay of Bengal and Arabian Sea. Apart from that, for validation of the model, field observations of water levels due to past cyclone induced storm surge events are also required. Table 8.3 summarizes the data requirements, possible sources and availability of such data for the present study.

The accuracy of inundation modeling depends to a large extent on the resolution of topographic data used; however, owing to non-availability of high-resolution LIDAR or sufficiently high resolution land-based survey maps, coarse resolution satellite based elevation data (ASTER) have been used for the Northern and Eastern Coastlines. Moreover, due to the same reason, the zero line/land line of the Northern and Eastern provinces were digitized from either those given in the navigation charts or from Google Earth.

Table 8.3 List of data requirements and availability.

Type of data	Source	Spatial resolution	Availability
Bathymetric data			
• Entire Indian Ocean Basin	GECBO	30 arc -seconds	Available
• Seaboard off Sri Lanka	Navigation charts	1:50.000 1: 300,000	Available
• Local Bathymetry	Navigation charts	1:10,000 1:15,000	Available at some locations
Elevation data for Coastal zone of Sri Lanka			
• LIDAR	DMC	Horizontal<1 m Vertical < 0.3 m	Available for coastline from Kalpitiya through Galle to Potuvil except between Ja-Ela to Moratuwa
• Land based surveys	Survey Department of Sri Lanka	1:50,000 1:1000, 1:5000, 1:10,000 (at least 1 m contour interval)	Available Limited Availability
• ASTER	JPL, Caltec	Horizontal = 30 m Verticval resolution not known	Available
Miscellaneous base data			
• Administrative boundaries in vector format	Survey Department of Sri Lanka	1:50,000, 1:10,000 or better	Available
• Vector data depicting land use types, drainage network, road network, etc	-ditto-	-ditto-	Limited Availability
Past cyclone events			
• Best track data	UNISYS, JTWC, IMD, SMRC, DMSL	N/A	Available (pre 1945 data availability sparse)
Data on past events of storm surges			
• Surge heights	Scientific Publications	Varying	Available (Limited in extent)
• Extent of inundation	Scientific Publications	-ditto-	Not Available

8.3.2 Statistical Analysis & Scenarios

A database of historical tropical cyclone events was compiled for the North Indian Ocean (NIO) region for the period 1900-todate using 'best-track' data from several sources including Joint Typhoon Warning Centre (JTWC) as indicated in Wijetunge (2011) of the US Navy and SAARC Meteorological Research Center (SMRC) as indicated in SAARC, 1998.

An observation window or a 'scanbox' bounded by 4-11° N & 78-93° E covering probable cyclone generation and feeder regions in southern portions of both Bay of Bengal and Arabian Sea was demarcated and all cyclones that had either formed or crossed the scan box during the above period were considered to have the potential to make landfall in or in the vicinity of Sri Lanka provided that necessary atmospheric forcing satisfied the requirements for the same (Wijetunge, 2011).

Of the subset of 201 independent cyclone events found to be falling within the scan-box mentioned above, the portion of the data prior to satellite observations (i.e., 1945), as well as those events for which it was not possible to assign reliable maximum wind speeds were excluded. Accordingly, the peak annual wind speeds corresponding to the remaining 59 independent cyclonic events were then statistically analyzed using Gumbel's method (Gumbel, 1958 & Holmes, 2007), following Rupp and Lander (1966) for tropical cyclones in Guam, and several others. The fact that, of the 201 cyclonic events in the database since 1900, only about 8% have made landfall in Sri Lanka was also incorporated into the probabilistic analysis by employing the multiplication rule. Fig. 8.5 shows the resulting plot of wind speed against the reduced variate: the intercept and the slope of the linear regression line give the mode (u = 32.26) and slope (a = 11.68) of the fitted Type-I extreme value distribution (Wijetunge, 2011).

The recurrence interval for different wind speeds could thus be deduced, and accordingly, the following scenarios were selected for the storm surge hazard assessment:

1. Wind speed of 270 km/h with an estimated recurrence interval of 300 years (Scenario-1);
2. a wind speed of 215 km/h with an estimated recurrence interval of 90 years (Scenario-2);
3. a wind speed of 160 km/h with an estimated recurrence interval of 30 years (Scenario-3); and
4. a wind speed of 110 km/h with an estimated recurrence interval of 10 years (Scenario-4).

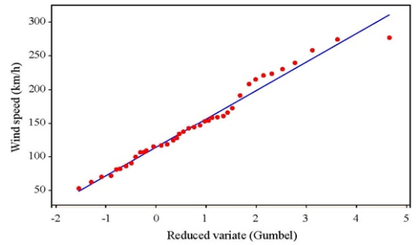

Fig 8.5 Analysis of annual maxima of cyclonic wind speeds using the Gumbel method.

8.3.3 Numerical Modelling of Cyclonic Surges

MIKE 21 Flow model, a numerical modeling system developed by DHI Water and Environment, was used to predict the sea surface elevation due to cyclone induced wind and pressure fields. Numerical simulation of cyclone driven storm surges was carried out in two stages in the MIKE21 model. First, the model simulates the cyclone generated space- and time-varying wind and pressure fields,

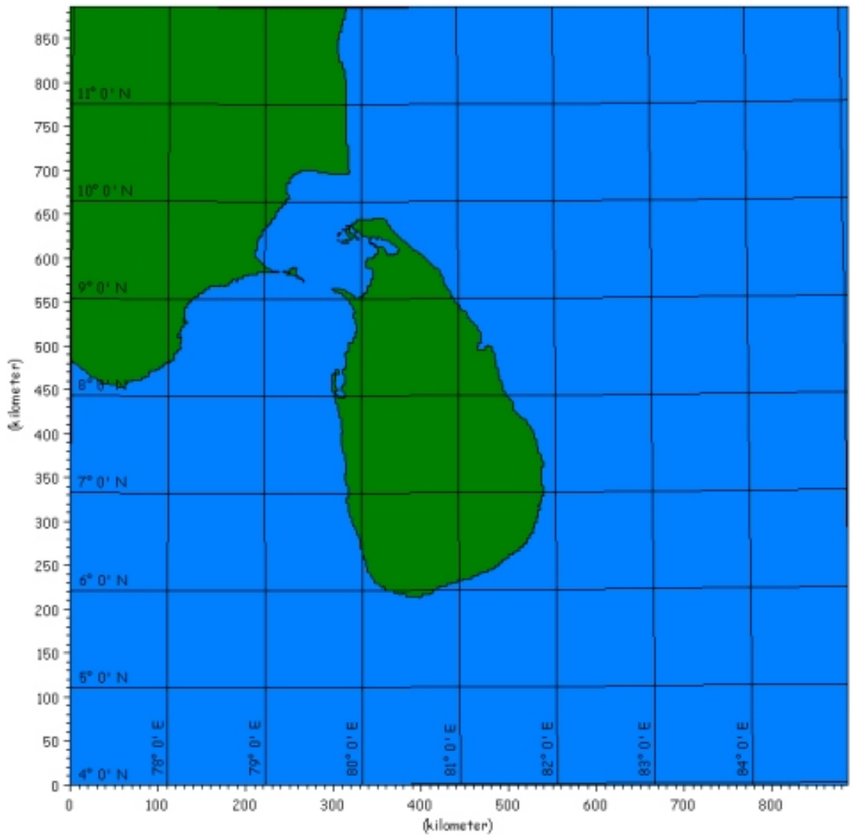

Fig 8.6 Computational domain used for cyclone and storm surge simulations

and secondly, MIKE21 HD, the hydrodynamic model, employs the wind and pressure fields as the forcing for the storm surge simulations. MIKE 21 Flow model has been successfully applied in many previous studies of cyclone induced storm surges, and has also been approved by the US Federal Emergency Management Agency (FEMA) for coastal storm surge modeling since 2001. Details of modeling & data analysis are given in original report published in DMC web site.

8.3.4 Storm Surge Propagation Simulations

8.3.4.1 Study Area and Grid Set-up

The computational domain for the present study was selected based on consideration of past studies of storm surges in the NIO region covering Sri Lanka, for example, those of Henry et al (1992). and Chittibabu et al.(2002). Accordingly, a rectangular region extending from 77°E - 85°E and 4°N - 12°N was selected (Fig. 8.6).

The bathymetry for the computational grid of 2 km spatial resolution was at first interpolated

from GEBCO data and was then updated with data from navigation charts. These navigation charts typically covered depths down to about 3000–4000 m at scales 1:150,000 or 1:300,000. Supplementary high resolution bathymetric data at scales of 1:10,000 and 1:15,000 were also used to further refine several near shore localities off port cities such as Galle, Colombo and Trincomalee. The depths in navigation charts were reduced from Chart Datum (i.e., Lowest Astronomical Tide) to Mean Sea Level (MSL).

8.3.4.2 Model Verification

Available information relating to the following past cyclones that made landfall in Sri Lanka were used to calibrate and verify the storm surge model set-up developed for the present hazard assessment.

- 1964-cyclone
- 1978-cyclone
- 1992-cyclone

The computed surge heights corresponding to each of the above cyclone induced storm surge events are given below.

Cyclone of 1964

The cyclone of 1964 made landfall on the Sri Lankan coast on 22nd December, 1964 at 0600 UTC at a location about 50 km north of Trincomalee. The cyclone then travelled northwest and crossed the coast north of Mannar, preceded to Tondi and Rameswaram in Tamil Nadu in the afternoon of 23rd December, before weakening and moving into the Arabian Sea (Fig. 8.7). The reported maximum wind speed associated with this cyclone was 60 m/s[8].

The simulation of this cyclone was carried out for the time period between 22/12/1964 00:00 UTC and 23/12/1964 00:00 UTC (Fig. 8.8 illustrates snapshots of the simulation). The model is integrated with a pressure drop of 60 hPa and a radius of maximum wind speed of 30 km.

The Maximum Envelope of Water (MEOW), which gives the highest surge elevation at each grid point throughout the simulation period, is shown in Fig. 8.9. It can be seen in Fig. 8.7 that there had been considerable surge along the northern and north-western coasts of Sri Lanka and also along a part of the southwest coast of India.

The computed peak surge heights at water points nearest the shoreline of (a) North coast, (b) East coast, and (c) Northwest coast due to 1964-cyclone are shown in Fig. 8.10. The surge elevations along the northern coastline are higher

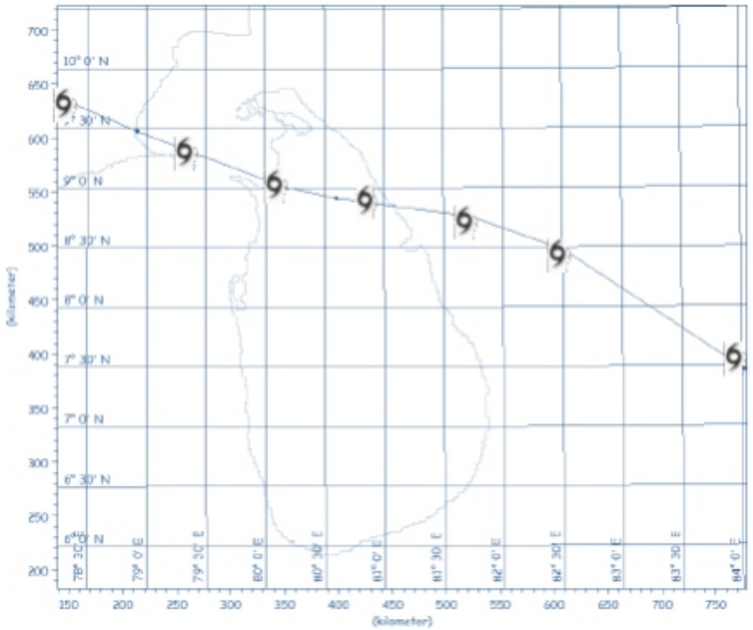

Fig. 8.7 The track of 1964-cyclone

compared to the east coast with the highest surge of about 4.5 m occurring near Mannar.

A maximum surge of about 5.4 m is computed near Tondi, while the north-east coast of Sri Lanka, and experiences a 1-2 m surge. Moreover the maximum surface elevation near Rameswaram and Pamban is 3-4 m and that in the coastal stretch between and Madampan and Nagapattinam is 2-3 m.

Cyclone of 1978

The 1978 cyclone crossed the coast of Sri Lanka near Batticaloa on the night of 23rd November, 1978. The storm retained its hurricane intensity till it emerged into the Gulf of Mannar, moved south of Pamban, crossed Tamil Nadu coast of India on 24th evening as a severe storm and emerged into the Arabian Sea off Kerala coast as a deep depression on the 25th morning (Fig. 8.11).

The numerical simulation of the storm surge due to the 1978-cyclone was carried out for the time period between 23/11/1978 0300 UTC and 24/11/1978 1200 UTC with a pressure drop of 50 hPa and a radius of maximum wind of 30 km. Fig 8.12

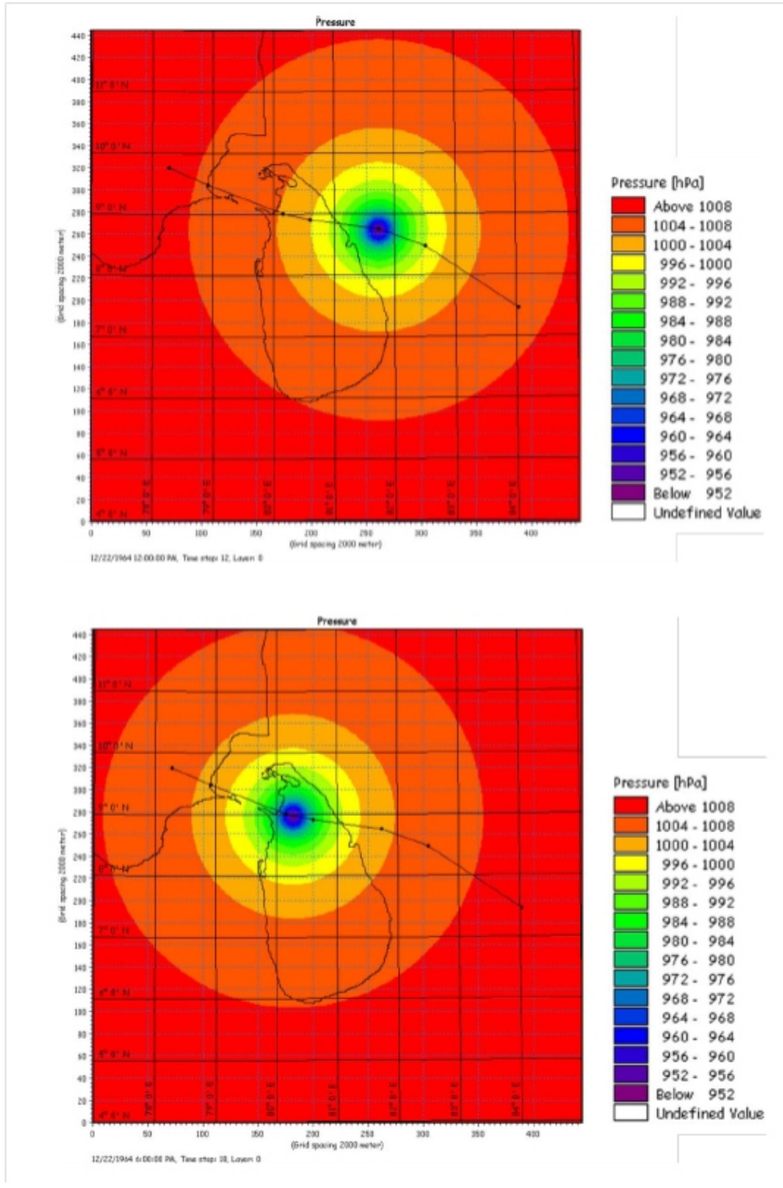

Fig 8.8 Snapshots of pressure field computed by MIKE21 cyclone model.

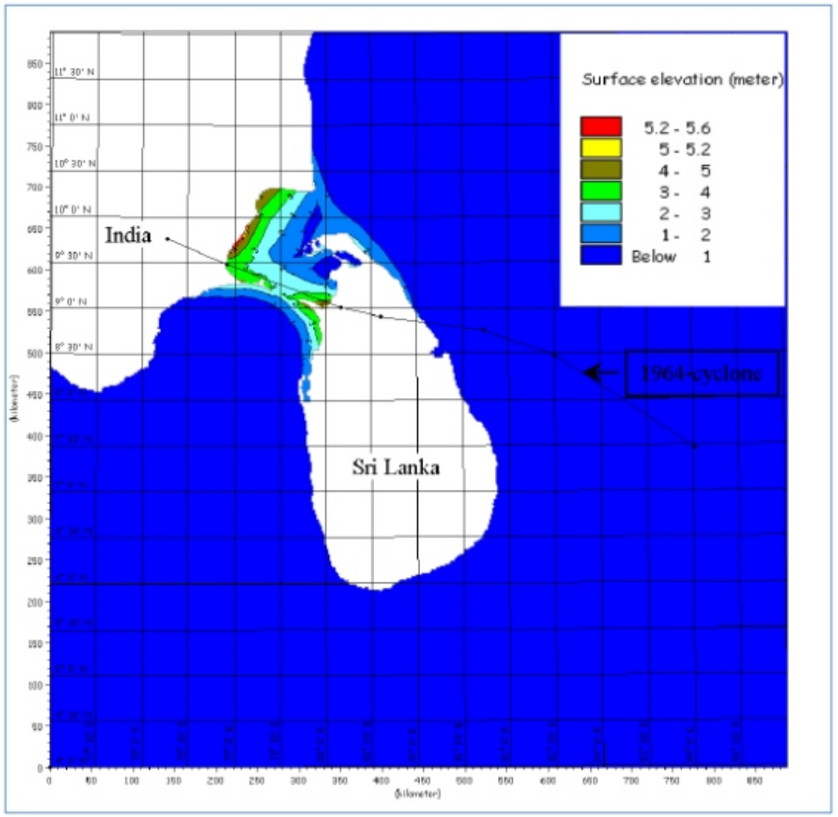

Fig 8.9 Computed maximum surge heights due to the passage of 1964-cyclone.

illustrates the computed maximum surge heights due to the passage of 1978-cyclone. Fig 8.13 illustrates the computed peak surge heights at water points nearest the shoreline of (a) North coast, (b) East coast, and (c) Northwest coast due to 1978-cyclone

Cyclone of 1992

The 1992-cyclone formed as a deep depression near (87.2°E, 7.5°N) at 0300 UTC on November 11th, then intensified into a cyclonic storm near (85.2°E, 7.5°N) at 0900 UTC on the same day. The cyclonic storm then moving in a westerly direction across Sri Lanka, emerged into Gulf of Mannar on 13th morning before further intensifying into a severe cyclonic storm on the same day and crossing South Tamil Nadu coast near Tuticorin on the Evening of November 13th (Fig 8.14).

The simulation was done for the time

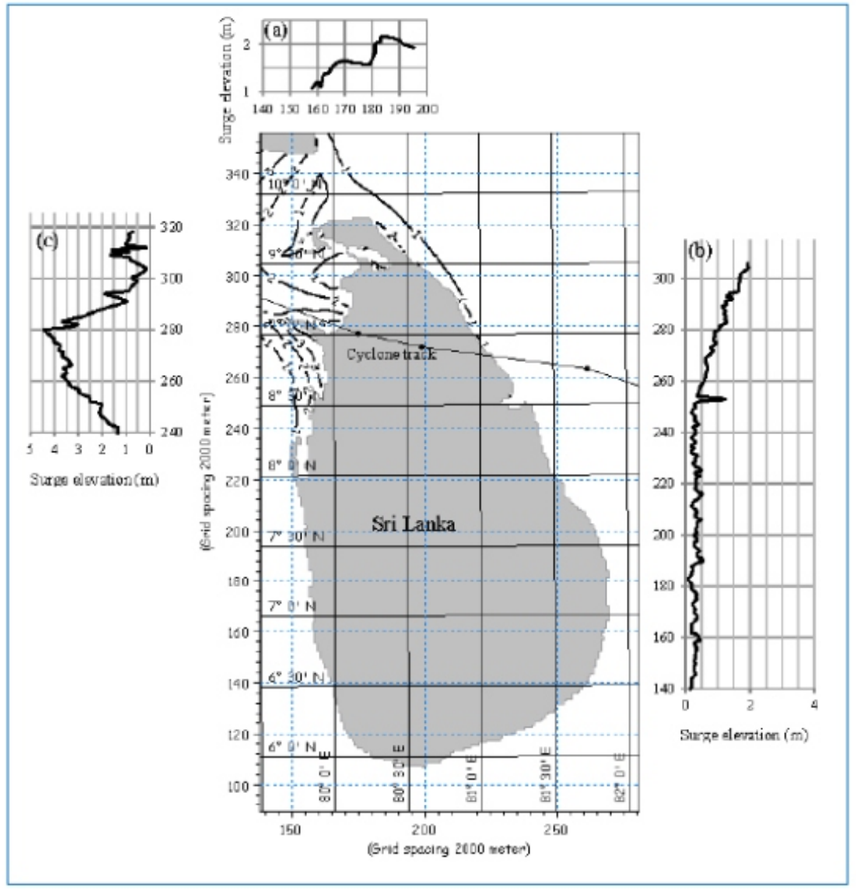

Fig 8.10 Computed peak surge heights at water points nearest the shoreline of (a) North coast, (b) East coast, and (c) Northwest coast due to 1964-cyclone.

period between 11/11/1992 12:00 UTC and 13/11/1992 12:00 UTC with a pressure drop of 40 hPa and a radius of maximum wind of 28 km. Fig 8.15 illustrates the computed maximum surge heights due to the passage of 1992-cyclone. Fig 8.16 illustrates the computed peak surge heights at water points nearest the shoreline of (a) North coast, (b) East coast, and (c) Northwest coast due to 1992-cyclone.

8.3.5 Comparison with Observed Surge Levels

The verification of storm surge model simulations was performed by comparing the computed peak surge heights with those observed at several locations (Table

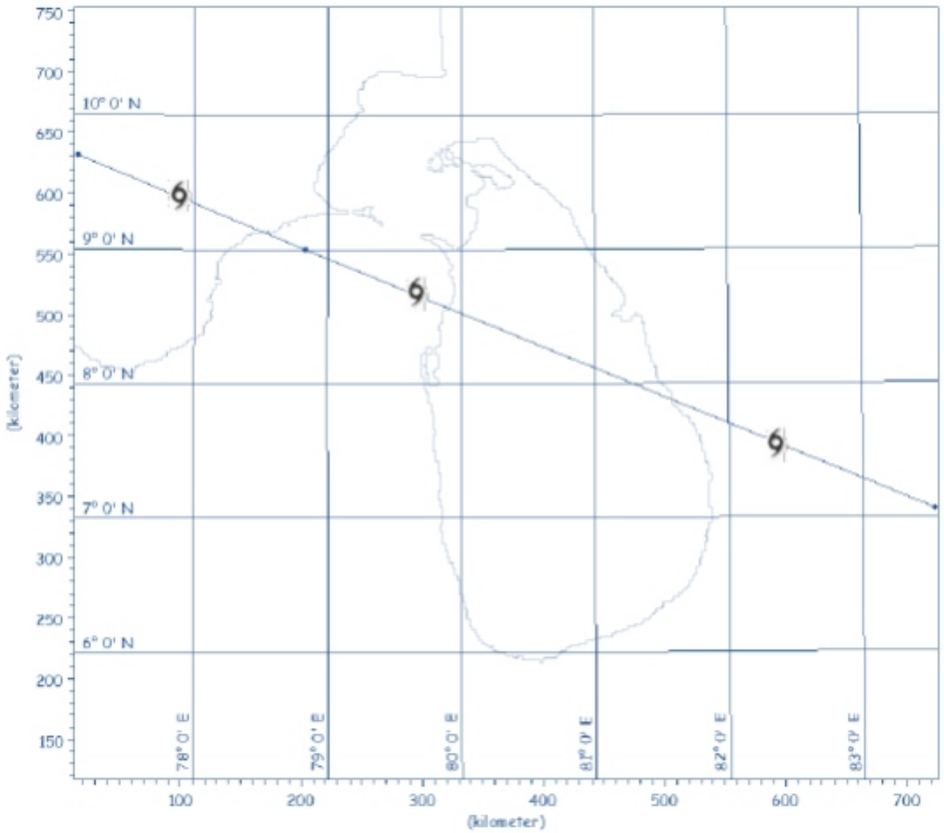

Fig 8.11 The track of 1978-cyclone.

8.4; locations marked in Fig. 8.17). As indicated in Table 8.4 that the ranges of simulated surge values on the whole give good agreement with the respective observed surge heights, thus verifying the suitability of the present model set-up to simulate cyclone scenarios for the purpose of storm surge hazard assessment.

8.3.6 Mapping

8.3.6.1 Mapping Scales

Table 8.5 gives the mapping scales decided to review the methodology for hazard mapping, based on UNDP/GRIP guidelines, resolution of inundation simulations as well as user requirements. Accordingly, district level storm surge hazard maps were developed at a scale of 1:50,000. These maps are available in the DMC web site.

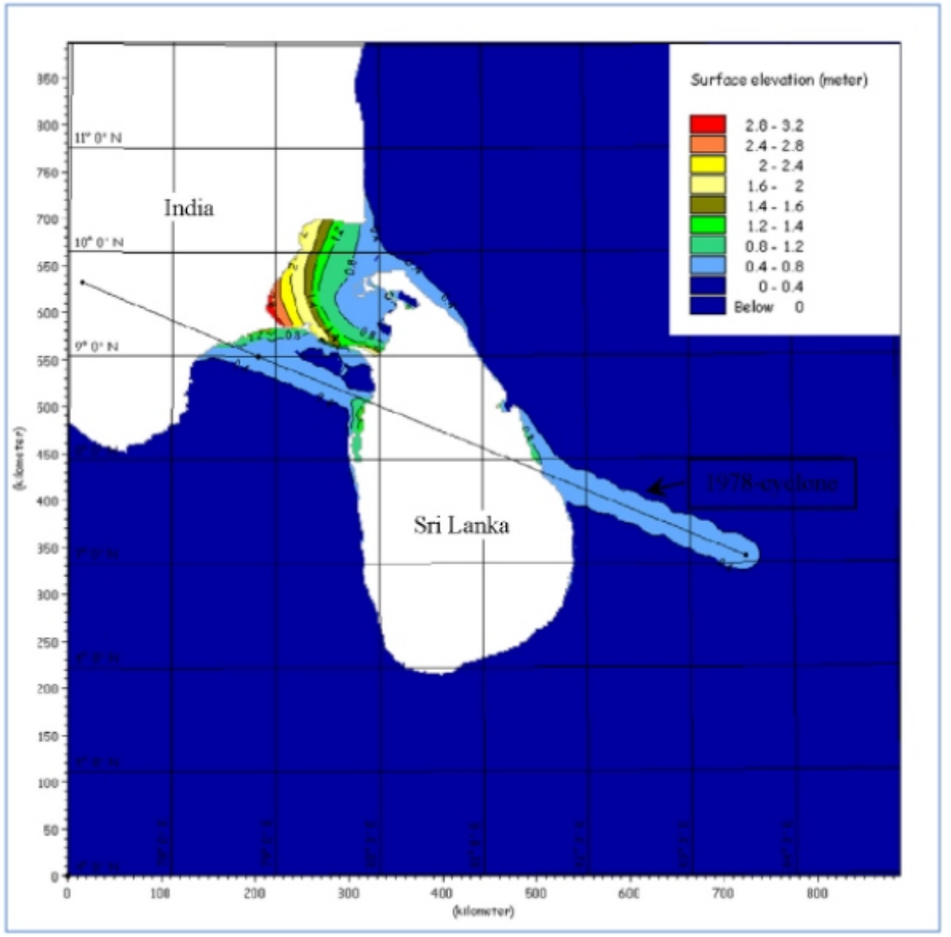

Fig 8.12 Computed maximum surge heights due to the passage of 1978-cyclone.

8.4 Hazard Profile

The storm surge hazard maps will be useful for future short term & long term planning to prevent the impacts of storm surge on people living in coastal regions. The maps produced will help to locate the potential sensitive areas & for the responsible stakeholders to give the warning signals to people living in such sensitive areas prior to receiving of whether reports on cyclonic condition closer to Sri Lanka.

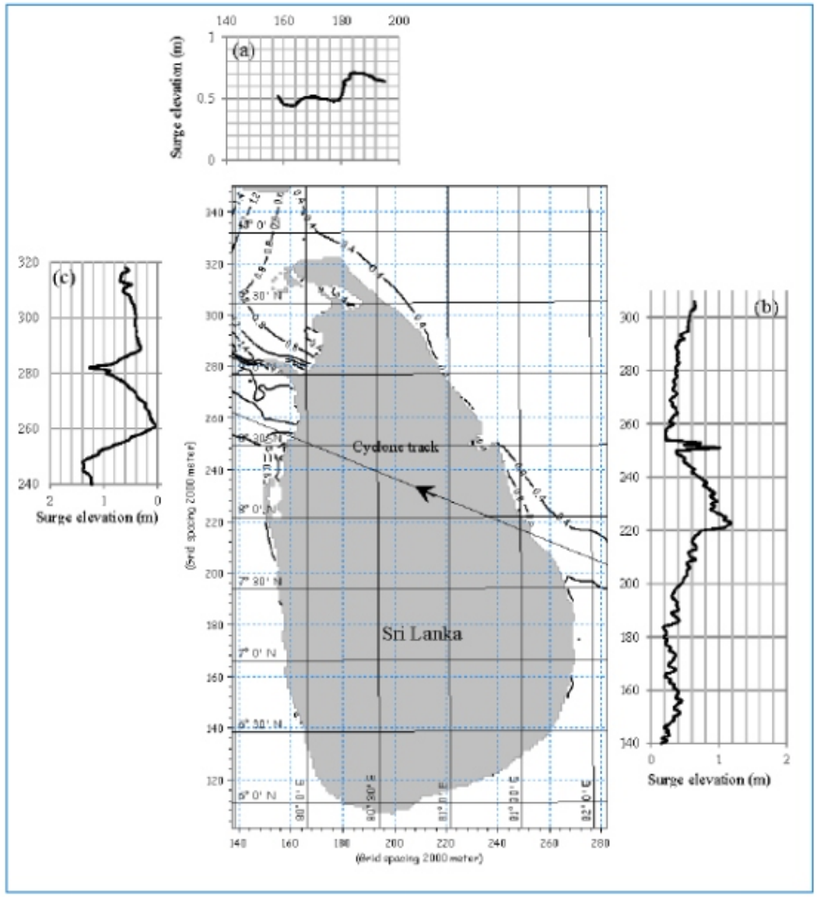

Fig 8.13 Computed peak surge heights at water points nearest the shoreline of (a) North coast, (b) East coast, and (c) Northwest coast due to 1978-cyclone.

8.4.1 Simulation of Hazard Scenarios

The following cyclone scenarios together with respective recurrence intervals (Table 8.6 have been derived for storm surge hazard assessment based on the statistical analysis carried out. Scenario-1 may be termed as the worst-case scenario whilst scenario-2 a long-term event, scenario-3 a medium-term event, and scenario-4 a short-term event.

As there is considerable uncertainty on the probable cyclone tracks including the landfall location, the storm surge simulations for each scenario was carried out for a large set of synthetic tracks that

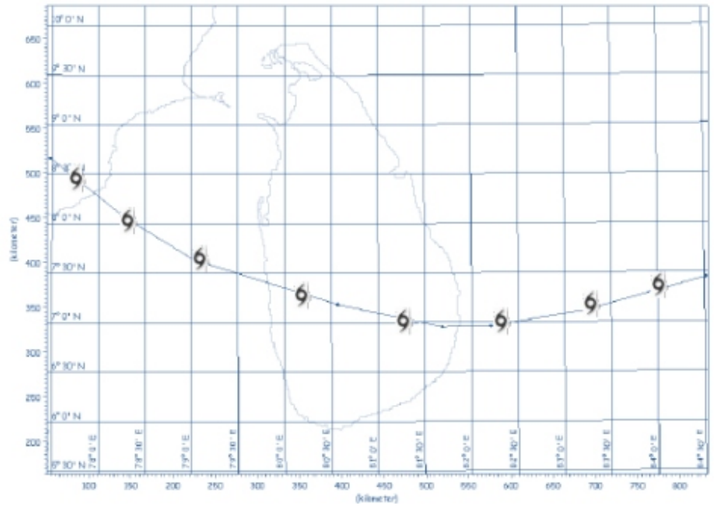

Fig 8.14 The track of 1992 cyclone.

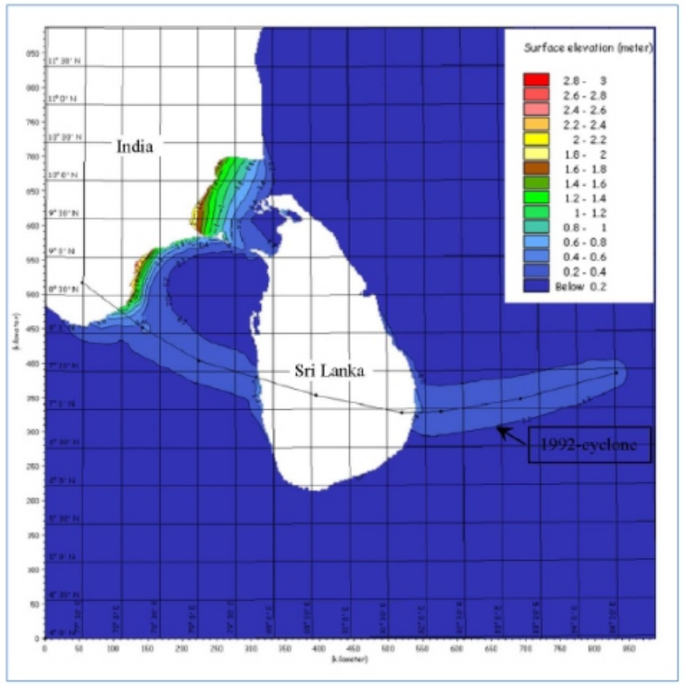

Figure 8.15 Computed maximum surge heights due to the passage of 1992-cyclone.

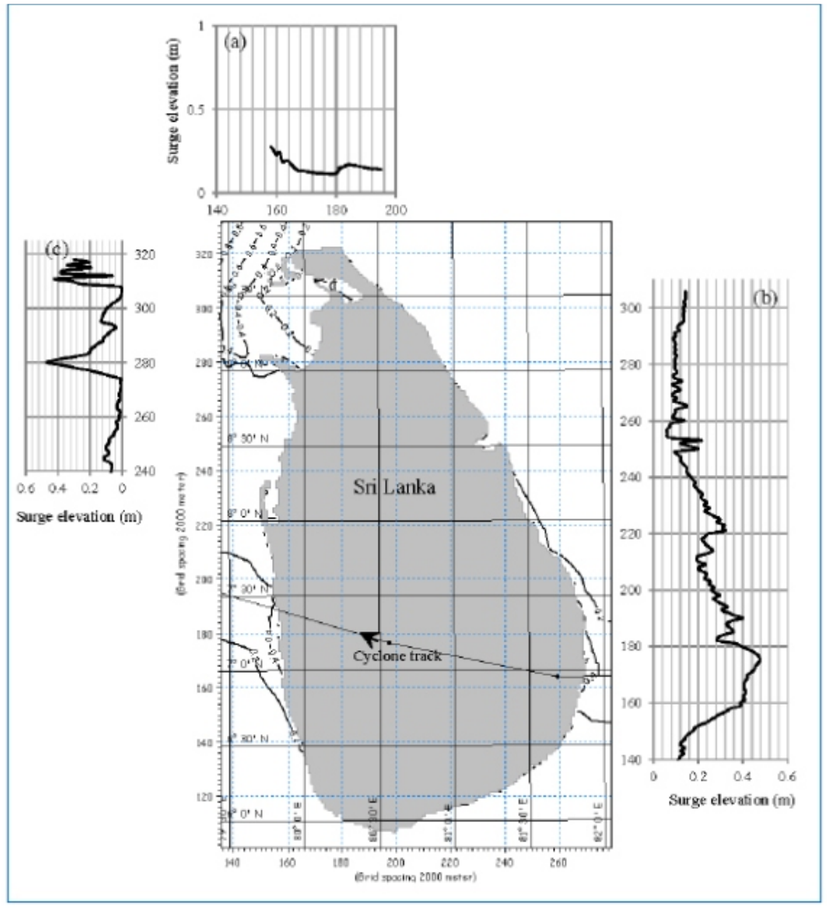

Fig 8.16 Computed peak surge heights at water points nearest the shoreline of (a) North coast, (b) East coast, and (c) Northwest coast due to 1992-cyclone.

are in statistical agreement with the historical database (e.g., as in Emanuel et al (2010). and Hallegatte (2007). Accordingly, for each scenario, the landfall location on the coastline was varied at 0.182o (~20 km) intervals along the latitude and an array of separate model simulations was carried out for each hypothetical track. The models for cyclone scenarios-1 and -2 were integrated with a maximum pressure drop of 80 hPa and a radius of maximum wind of 40 km. The model for cyclone scenario-3 was integrated with a maximum pressure drop of 70 hPa and a radius of maximum wind of 35 km whilst these parameters for scenario-4 were 60 hPa and 35 km, respectively.

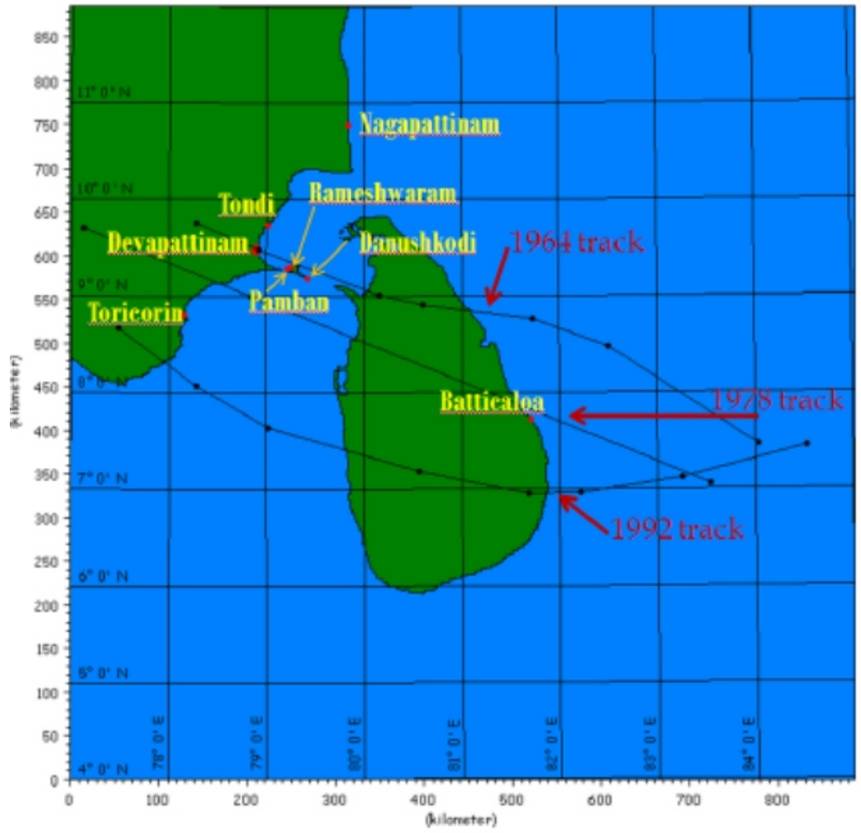

Fig 8.17 Locations where observed surge elevations are compared with computed values in Table 5.3.

The computed maximum surge heights at every grid point corresponding to each of the above hazard scenarios was collated to form composite maps of peak surges over the entire model domain (Figs 8.18-8.21). Note that the surge levels shown in Figs 8.18- 8.21 for wind speeds, (a) 270 km/h, and (b) 215 km/h, are exclusive of tidal effects. For a conservative, worst-case estimate of storm tide, an additional 0.3 m may be added to the surge levels shown in Figs 8.18-8.21.

8.4.2 Uncertainties Associated with Observed and Computed Surge

Uncertainties associated with computed surge:

Non-consideration of wave setup

Wave setup consequent to breaking, although comparatively low, has not been included in the present analysis.

Table 8.4 Comparison of computed surge heights with observations. The respective sources of information relating to observed heights are given in brackets.

Cyclone	Location	Surge Height Observed	Simulated
1964	Rameswaram	3-4.2 m[21]	3.0-4.0 m
	Pamban and Nagapattinam coastal stretch	3-5 m[21]	3.0-3.7 m
	Tondi	3-6 m[11]	3.2-5.8 m
	Dhanushkodi	3-6 m[8]	2.8-3.4 m
	Mannar	4.5 m[22]	4.8-5.2 m
1978	Coastal areas between Tondi and Devipattinam	3-5 m[8]	2.4-3.3 m
	Batticaloa	1-2 m[21]	0.8-1.6 m
1992	Tuticorin	1-2 m[11]	2.3-3.0 m

Table 8.5 Mapping scales.

Mapping Level	UNDP/GRIP Guidelines +	Adopted*
City/ Municipality	1:5,000 – 1:25,000	1:10,000
District	1:25,000 – 1:100,000	1:50,000

UNDP/GRIP National Risk Assessment- Tools and Guidelines25.
** As decided at the Technical Group Meeting held on 5th April 2010 to review the methodology for hazard mapping.*

Effect of land boundary

In model setup, the land boundary behaves as a vertical wall, so the surge at the land boundary tends to amplify. This condition may give a higher value than the actual surge causing inundation.

Effect of rainfall

In case significant rainfall is associated with the cyclone, which is common, the surge elevations could be higher owing to the increased volume of water.

Input model parameters such as wind speed

The computed surge heights are highly dependent on the rotational speed of the cyclone; however, typical uncertainties within measuring cyclone speeds leads to uncertainties with the simulated surge elevations.

Uncertainties associated with observed surge:

Location of surge observed Since observations of surge levels have been made onshore, observed values depend on the topography of the location. Therefore, an uncertainty arises as to whether the observed values are with respect to the mean sea level, or the flow depth with respect to the ground elevation at that location. Moreover, locations of measured surges were identified with the name of the closest city, so the simulated values may not have been extracted at exactly the same locations, although quite likely in the vicinity.

Time of surge observed

It was assumed that the observed surges are the maximum values at the respective locations although this need not necessarily be so.

Tide at the time of observations

The time at which observations have been made is not known, and therefore, it is impossible to filter out the tide when comparing with computed values exclusive of the tide.

8.4.3 Hazard Assessment Maps Corresponding to Different Cyclone Scenarios

Figs 8.18 to 8.21 illustrate the composite maps of peak surge heights corresponding to different cyclone

Table 8.6 Cyclone hazard scenarios.

Scenario	Maximum Wind Speed	Estimated recurrence interval	The probability of this event occurring in the next 25 years
worst-case scenario	270 km/h	300 years	8%
long-term even	215 km/h	90 years	25%
medium-term event	160 km/h	30 years	57%
short-term event	110 km/h	10 years	92%

scenarios with an estimated recurrence interval of 300, 90,30 and 10 years. A key map is provided for 1:50000 detailed maps prepared for the same and it is published in DMC web site for references.

8.4.4 Spatial Distribution of Inundation

Figs 8.22 and 8.23 show tropical cyclone induced inundation distribution at high tide corresponding to scenarios-1 and -2, respectively. Following, the classification of flow depths adopted for tsunami hazard maps, the computed storm surge inundation distribution is shown on the maps in three color-coded depth ranges: less than 0.5 m, 0.5–2 m, and greater than 2 m, corresponding to low, medium and high levels of the hazard, respectively.

Layers depicting water bodies and waterways should be added to these maps. Clearly, north and east coasts are more prone to the cyclone induced storm surge hazard with the north-western coastline including the coastal areas of Mannar and Jaffna peninsula particularly exposed.

8.5 Conclusions

North and east coasts are more prone to the cyclone induced storm surge hazard with the north-western coastline including the coastal areas of Mannar and Jaffna peninsulas are particularly exposed.

8.6 Recommendations

The results of the present storm surge hazard assessment are intended for use in coastal disaster risk mitigation planning, evacuation planning and in public education and awareness activities only. The hazard maps for scenario-1 may be more appropriate for use in evacuation planning whilst those for scenario-2 are probably more suitable for medium- to long-term disaster risk mitigation planning. Because of the uncertainties inherent in this type of modelling, these results are, however, not intended for land-use regulation. The storm surge hazard maps and the information presented therein are also not legal documents and should not be used for any regulatory purpose.

Even though this document does not recommend using the information for

landuse planning, it could be used as a baseline document to develop future landuse planning in coastal areas. Also it could be used to propose short term & long term mitigatory measures to minimize the impacts of storm surge on potential coastal areas & on coastal populations.

8.6.1 Recommendations for Improving the Hazard Maps

The accuracy of inundation simulations for northern and eastern provinces could be improved by utilizing higher resolution topographic data such as those acquired through the LIDAR system. It is also desirable to carry out ground verifications to detect any discrepancies, particularly in the northern and eastern provinces, since the vertical resolution of elevation data (ASTER) utilized in the present inundation simulations for the north and east is coarse.

The present version of the maps could be further enhanced by incorporating more information relating to the storm surge hazard and mitigation measures. Details of the map descriptions are given in the website together with the 1: 50,000 maps.

8.7 Limitations

One limitation is that the resolution of the modelling is no greater or more accurate than the bathymetric and topographic data used. Non availability of higher resolution topographic data for the north and east coasts was a major limitation. The resolution of the model also constrains its ability to resolve some small-scale features of the onshore terrain including narrow waterways. Moreover, the tide has been linearly superimposed on the computed storm surge levels on a conservative basis although the tide-surge interaction is non-linear. It must also be added that set-up due to wave breaking, storm rainfall, riverine flooding, ground cover and variations in surface roughness have not been incorporated in the present model simulations.

The depth-averaged models assume a uniform velocity profile across the flow depth and neglect vertical accelerations. Moreover, the mathematical formulation employed in the present model does not explicitly account for all means of energy dissipation for a flood wave surging onshore over an urban landscape. For instance, although energy dissipation due to bottom friction is included in the present model, dissipation due to turbulence is not explicitly formulated.

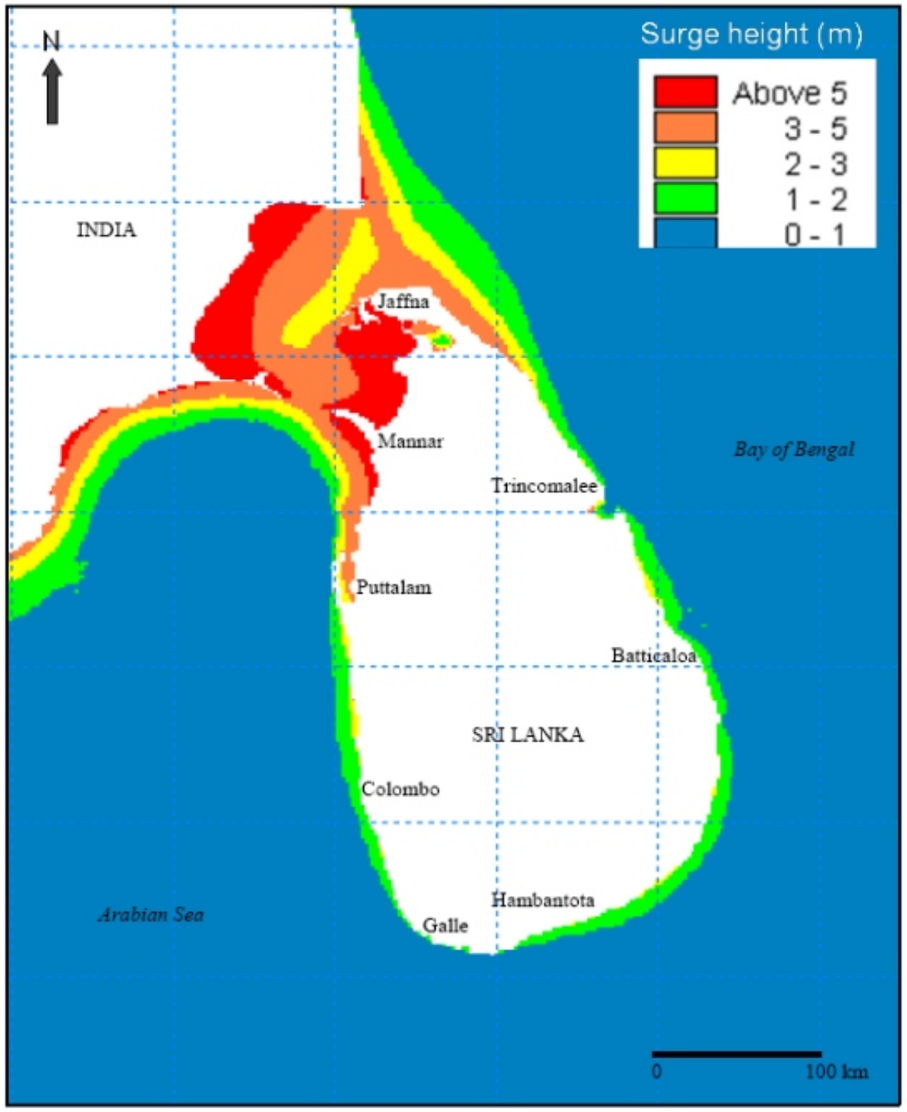

Fig 8.18 Composite map of peak surge heights corresponding to cyclone scenario-1 (max. sustained wind speed = 270 km/h) with an estimated recurrence interval of 300 years.

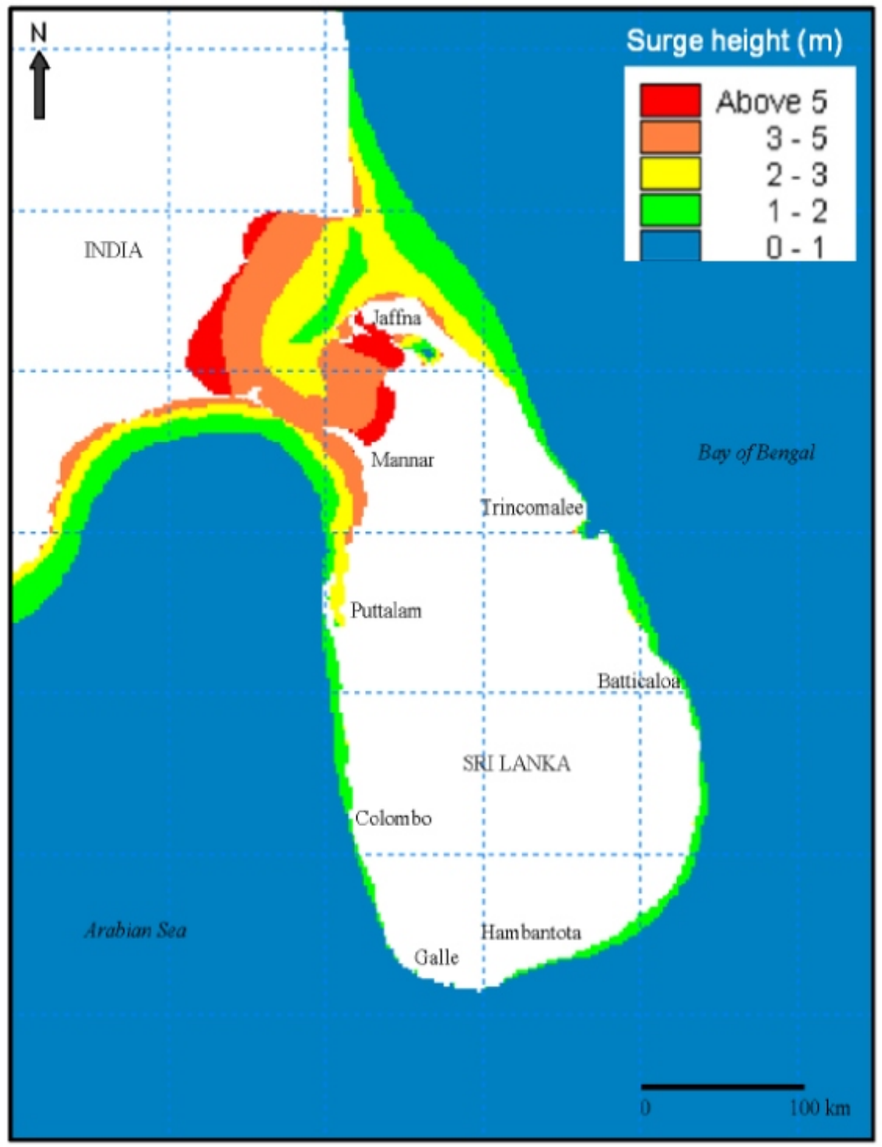

Fig 8.19 Composite map of peak surge heights corresponding to cyclone scenario-2 (max. sustained wind speed = 215 km/h) with an estimated recurrence interval of 90 years.

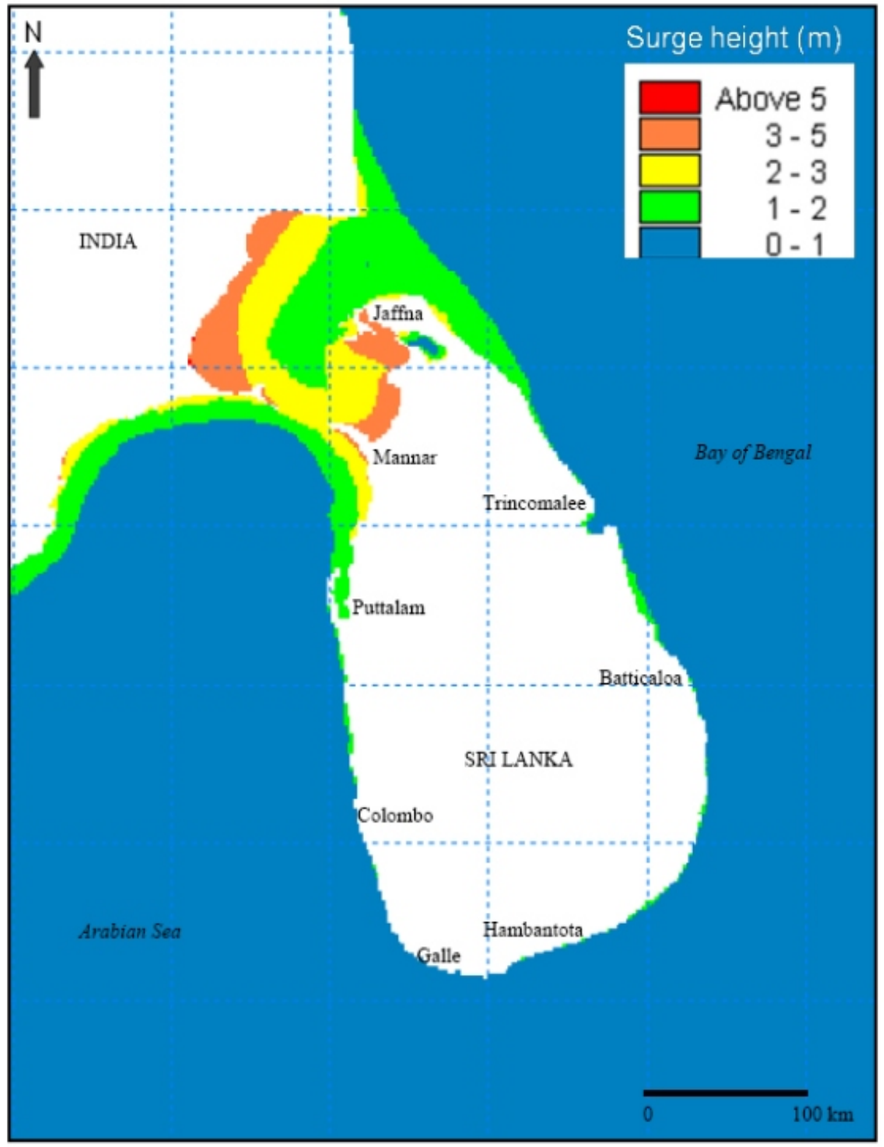

Fig 8.20 Composite map of peak surge heights corresponding to cyclone scenario-3 (max. sustained wind speed = 160 km/h) with an estimated recurrence interval of 30 years.

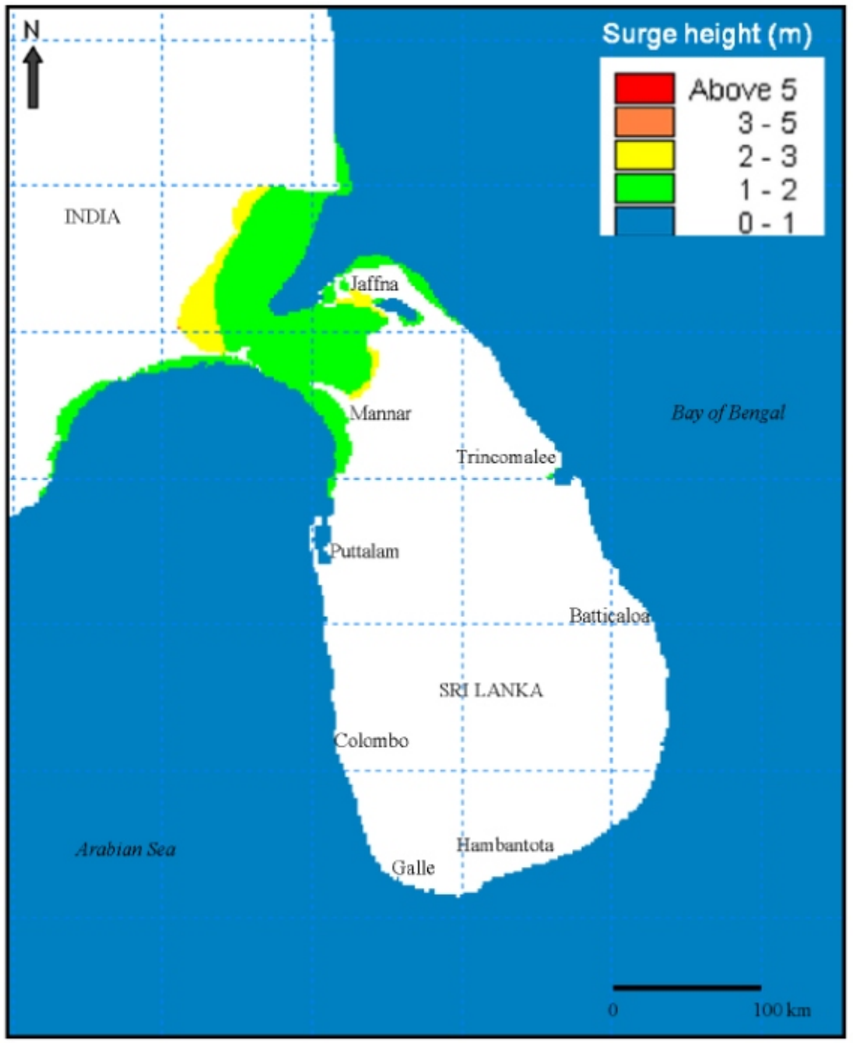

Fig 8.21 Composite map of peak surge heights corresponding to cyclone scenario-4 (max. sustained wind speed = 110 km/h) with an estimated recurrence interval of 10 years.

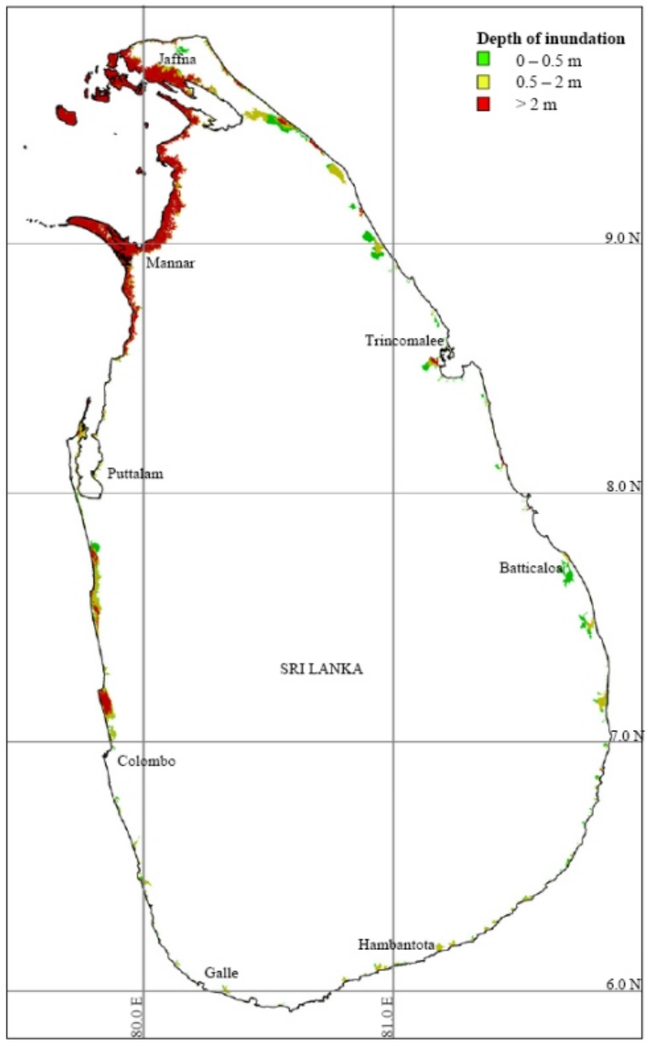

Fig 8.22 Tropical cyclone induced storm surge inundation corresponding to scenario-1.

CHAPTER 08

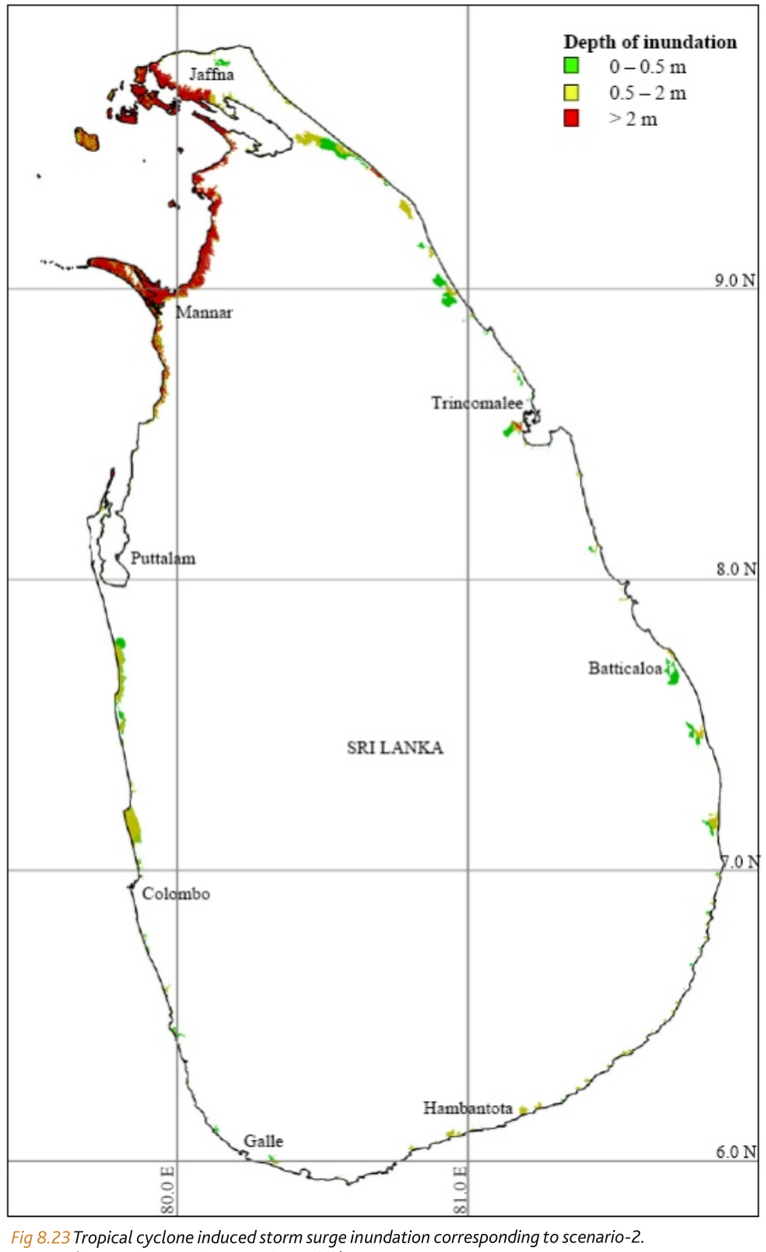

Fig 8.23 Tropical cyclone induced storm surge inundation corresponding to scenario-2. (for detail map refer; www.hazard.lk)

8.8 References

Ceylon Daily Mirror (1964). Ceylon Daily Mirror Newspaper of 29 December, 1964, Colombo.

Chittibabu, P. , Dube, S. K. , Sinha, P. C. , Rao, A. D. and Murty, T. S.(2002) 'Numerical Simulation of Extreme Sea Levels for the Tamil Nadu (India) and Sri Lankan Coasts, Marine Geodesy, 25(3): 235-244.

Department of Meteorology, Sri Lanka (2010). Tropical cyclones; Cyclone events 1900-2000, Department of Meteorology, Government of Sri Lanka, http://www.meteo.gov.lk/, accessed on 15-6-2010.

Dube, S.K. (2003). Storm surge forecasting in the Bay of Bengal and Arabian Sea. In Antarctic Geoscience, Ocean-Atmosphere Interaction and Paleoclimatology (Eds. S. Rajan and P.C. Pandey), National Centre for Antarctic & Ocean Research, Goa, India.

Emanuel, K. and Jagger, T. (2010). On estimating hurricane return periods. J.Appl. Meteorology and Climatalogy, 49: 837-844.

Gumbel, E.J. (1958). Statistics of Extremes. Columbia University Press, New York.

Hallegatte, S. (2007). The use of synthetic hurricane tracks in risk analysis and climate change damage assessment. Center for Environmental Sciences and Policy, Stanford University, USA.

Henry R.F. and T.S. Murty (1992). Storm surges and tides around Sri Lanka, Recent advance in Marine science and technology, 92:205-218.

Holmes, J. (2007). Wind loading on structures, 2nd Edition, Taylor & Francis, London.

IRI (2011). Identification of global disaster risk hotspots., Sri Lanka case study. http://iri.columbia.edu/~mahaweli/disaster/maps/cyclone.jpg.

Jelesnianski, C.P., Chen, J., and Shaffer, W.A. (1992). "SLOSH: Sea, Land and Overland Surges from Hurricanes", NOAA Technical Report, NWS 48, Silver Springs, Maryland.

Kariyawasam, S. H. (2005). Tropical cyclones, tornadoes. Vidurawa, 22(2) (Special Issue): 14-17.

Kulshrestha, S.M. and Gupta, M.G. (1966). Satellite study of the Rameswaram cyclonic storm of 20-23 December 1964. Journal Appl. Meteorology, 5(3): 373- 376.

Lin, N., K. A. Emanuel, J. A. Smith, and E. Vanmarcke (2010). Risk assessment of hurricane storm surge for New York City. Journal Geophys. Res., 115, D18121.

Longshore, D. (2008). Encyclopedia of Hurricanes, Typhoons, and Cyclones, Facts on File, New York.

Murty, T.S., Flather, R.A., and Henry, R.F. (1986). The storm surge problem in the Bay of Bengal. Prog. Oceanog., 16: 195-233.

Ramesh, R. (2004). Sethusamudram Shipping Canal Project and the unconsidered high risk factors: Can it withstand them? Doctors for Safer Environment, Coimbatore, Tamil Nadu.

Rupp, J. A. and Lander, M. A. (1996). A technique for estimating recurrence interval of tropical cyclone-related high winds in the tropics: Results from Guam. J. Ame. Met. Soc., May 1996: 627-637.

SAARC (1998). The impact of tropical cyclones on the coastal regions of SAARC countries and their influence in the region. Publication No. 1, SAARC Meteorological Research Centre (SMRC), Bangladesh.

Wijetunge, J. J. (2011). Progress Report No. 1, RG/2011/ESA/01, National Science Foundation.